iScience

CellPress
OPEN ACCESS

Article

Reversion of pathogenic *BRCA1* L1780P mutation confers resistance to PARP and ATM inhibitor in breast cancer

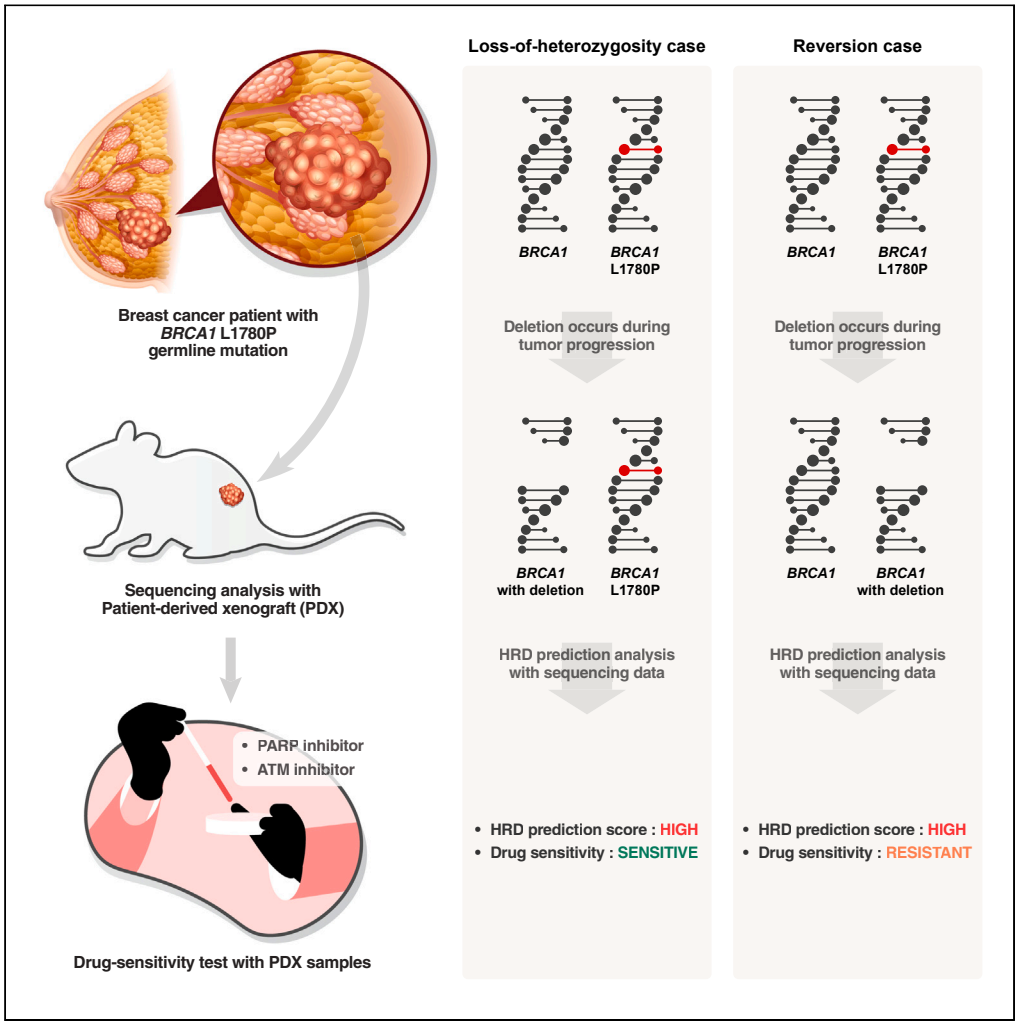

Se-Young Jo, Jeong Dong Lee, Jeongsoo Won, ..., Seung-Il Kim, Sangwoo Kim, Hyung Seok Park

swkim@yuhs.ac (S.K.)
imgenius@yuhs.ac (H.S.P.)

Highlights

PDX models of *BRCA1* L1780P showed opposing LOH

HRDetect and CHORD show a homologous recombination deficiency of *BRCA1* L1780P mutation

Reversion mutations exhibit drug resistance conflicts with HRD predictions

Understanding genomic dynamics is crucial for the prediction of accurate drug response

Jo et al., iScience *27*, 110469
August 16, 2024
https://doi.org/10.1016/j.isci.2024.110469

iScience

CellPress
OPEN ACCESS

Article

Reversion of pathogenic *BRCA1* L1780P mutation confers resistance to PARP and ATM inhibitor in breast cancer

Se-Young Jo,[1,2,9] Jeong Dong Lee,[3,4,9] Jeongsoo Won,[1,2] Jiho Park,[1] Taeyong Kweon,[2,5] Seongyeon Jo,[2,5] Joohyuk Sohn,[6] Seung-Il Kim,[7] Sangwoo Kim,[1,2,8,*] and Hyung Seok Park[7,10,*]

SUMMARY

This study investigates the molecular characteristics and therapeutic implications of the BRCA1 L1780P mutation, a rare variant prevalent among Korean hereditary breast cancer patients. Using patient-derived xenograft (PDX) models and cell lines (PDX-derived cell line) from carriers, sequencing analyses revealed loss of heterozygosity (LOH) at the BRCA1 locus, with one patient losing the wild-type allele and the other mutated allele. This reversion mutation may cf. resistance to homologous recombination deficiency (HRD)-targeting drugs such as PARP inhibitors (PARPi) and ATM inhibitors (ATMi). Although HRDetect and CHORD analyses confirmed a strong association between the L1780P mutation and HRD, effective initially, drug resistance developed in cases with reversion mutations. These findings underscore the complexity of using HRD prediction in personalized treatment strategies for breast cancer patients with BRCA1/2 mutations, as resistance may arise in reversion cases despite high HRD scores.

INTRODUCTION

Breast cancer is one of the most prevalent malignancies affecting women worldwide.[1] This disease displays remarkable heterogeneity, with its subtypes classified based on the presence or absence of specific receptors: estrogen receptor (ER), progesterone receptor (PR), and human epidermal growth factor receptor 2 (HER2).[2] One particularly aggressive subtype, known as triple-negative breast cancer (TNBC), lacks these receptors entirely and is characterized by aggressive clinicopathological features.[3–5] Despite advances in cancer treatment, many TNBC cases lack specific molecular targets suitable for targeted therapies, thereby posing challenges in effective management. Therefore, identification of appropriate molecular targets for the treatment of TNBC is required.[6–8] Importantly, the mutation frequency of breast cancer type 1 and 2 (*BRCA1/2*) genes in TNBC is higher than that in luminal and HER2-positive breast cancer cases.[9–11] Therefore, understanding the role of *BRCA1/2* pathogenic mutations in breast cancer can provide valuable insights into potential therapeutic avenues.

BRCA1/2 genes are important for deoxyribonucleic acid (DNA) double-strand break repair,[12,13] and their methylations or pathogenic mutations lead to the phenomenon known as "BRCAness".[14] This state significantly impairs the homologous recombination deficiency (HRD) and subsequent genomic instability.[15] Remarkably, the BRCAness in tumors can be a druggable target based on the principle of synthetic lethality.[16] Cancer cells with BRCAness are more reliant on alternative DNA repair mechanisms owing to their impaired homologous recombination repair. This reliance on compensatory repair pathways presents an opportunity for targeted therapy. Specifically, drugs like PARP (PARPi) and ATM inhibitors (ATMi) have been developed to selectively target HRD-driven tumors. PAPRi work by inhibiting PARP enzyme, which is involved in base excision repair, a pathway that compensates for defective homologous recombination in HRD cells.[17,18] Similarly, ATMi inhibitors target the ATM protein, crucial for detecting DNA damage and initiating repair mechanisms. In HRD cells, inhibiting ATM can lead to further disruption of repair pathways, ultimately inducing cell death.[19] However, not all *BRCA1/2* mutations result in HRD. Thus, precise prediction of HRD occurrence is critical in estimating drug sensitivity.

BRCA1 c.5339 T>C, p.L1780P (L1780P) missense mutation, a variant of unknown significance, had high prevalence among patients with breast cancer in Korea.[20–22] Subsequent studies lent further support to this germline mutation's significance, classifying *BRCA1* L1780P as

[1]Department of Biomedical Systems Informatics, Yonsei University College of Medicine, Seoul, Korea
[2]Brain Korea 21 PLUS Project for Medical Science, Yonsei University College of Medicine, Seoul, Korea
[3]Avison Biomedical Research Center, Yonsei University College of Medicine, Seoul, Korea
[4]Biomedical Research Institute, Seoul National University Hospital, Seoul, Korea
[5]Department of Medical Science, Yonsei University College of Medicine, Seoul, Korea
[6]Division of Medical Oncology, Department of Internal Medicine Yonsei University College of Medicine, Seoul, Korea
[7]Department of Surgery, Yonsei University College of Medicine, Seoul, Korea
[8]Postech Biotech Center, Pohang University of Science and Technology (POSTECH), Pohang, Korea
[9]These authors contributed equally
[10]Lead contact
*Correspondence: swkim@yuhs.ac (S.K.), imgenius@yuhs.ac (H.S.P.)
https://doi.org/10.1016/j.isci.2024.110469

a "likely pathogenic mutation" in the American College of Medical Genetics guidelines.[23] However, comprehensive functional studies on *BRCA1* L1780P missense mutation have not been performed yet.

To investigate the precise genomic dynamics and drug sensitivity associated with this mutation, we should expand our tissue samples to achieve a higher level of tumor purity, facilitating more accurate drug testing. Thus, we utilized a patient-derived model, which reliably emulates the genomic, transcriptomics, and physical attributes of cancer tissue[24–27] to obtain clear insights into the dynamics of *BRCA1* L1780P missense mutation and its potential therapeutic implications.

RESULTS

Sample preparation

We examined two patients with TNBC with *BRCA1* L1780P germline mutation who have received taxane-based neoadjuvant chemotherapy, identified at Severance Hospital, Seoul, South Korea (Table S1). Primary tumor tissues from these patients, named SBP60 and SBP77, were successfully used to create first-generation PDX (PDX F1) by grafting them into NOG mice. Subsequently, the PDX F1 tissues were passaged through two generations, resulting in the acquisition of PDX F2 and F3 tissues. For further validation and investigation, an additional step was taken with SBP77. From the PDX F3 tissue of this patient, a PDXDC was successfully established (Figure 1). DNA- (including whole genome sequencing [WGS] and whole exome sequencing [WES]) and RNA-sequencing data were generated for all three generations of PDX tissues and their corresponding primary tumor tissues, while the WES data were generated for PDXDC and FFPE samples. To eliminate potential contamination from mouse cells, proper mouse genome-derived sequencing read filtering was applied on every data generated from PDX (Table S2).[28] Additionally, SNP concordance analysis (Table S3)[29] confirmed that all PDX samples were robustly established without cross-contamination.

Genetic profiles of patients with BRCA1 L1780P

Mutational profiles of both samples were analyzed longitudinally from the primary tumor tissues to the PDX samples (Figures 2A and S1). Among the cancer-related genes listed on Cancer Gene Census (CGC), three rare-damaging germline mutations were identified in *BRCA1*, *OMD*, and *NCOR2* for SBP60. Conversely, SBP77 harbored four rare-damaging germline mutations, including *BRCA1*, *BRCA2*, *CHD2*, and *MLLT10*. Both patients had critical somatic mutations in the *TP53* gene, with SBP60 showing a frameshift insertion and SBP77 exhibiting a nonsense mutation. Other somatic mutations were also detected and remained well conserved from the primary tissue to the xenograft samples.

The presence of RNA sequencing data allowed us to assess whether the gene expression profiles observed in primary tumor tissue were preserved in the corresponding PDX tissues. Remarkably, we observed exceptionally high intra-sample correlations for 19,134 gene expression values, with a median Pearson's correlation coefficient (r) of 0.965 (Figure 2B, light-gray boxes). This finding indicates a strong similarity in gene expression patterns between the primary tumor tissue and the PDX tissues. Furthermore, the inter-sample correlation also notably high with a median Pearson's correlation coefficient of 0.826 (Figure 2B, dark-gray boxes). This was attributed to the fact that all samples originated from the same cancer type, sharing many genetic characteristics.

The copy number signal in the primary tissue data were significantly hindered due to its low tumor purity. However, the utilization of PDX proved to be highly beneficial, the tumor purity of PDX samples reached nearly 100% (Figures S2–S4), enabling clear identification of the copy number status in the PDX samples with a high level of concordance (Figure 2C). Both patients exhibited a high level of copy number aberrations across all chromosomes, indicating a significant lack of genomic stability. We observed a significant number of copy number losses involving entire chromosomal arms or even whole chromosomes, which likely contributed to the occurrence of loss of heterozygosity (LOH) events. One such example was chromosome 17, in which interesting LOH cases related to the *BRCA1* germline mutation were identified (Figure 2D). Both SBP60 and SBP77 displayed LOH within the *BRCA1* region, but intriguingly, in opposite directions. In the case of SBP60, we observed the loss of the wild-type allele of *BRCA1*, resulting in the homozygous presence of the *L1780P* mutation. In contrast, SBP77 experienced LOH in the opposite direction, losing the mutant allele, and retaining only the wild-type allele, the phenomenon referred to as a reversion mutation. Confirming the LOH status solely based on primary tumor data proved challenging, as the allele-frequencies were not as extremely biased as expected in LOH cases, primarily owing to the low tumor purity (Figure 2E). However, PDX provided an advantage of higher tumor purity, allowing us to observe the actual allele-frequencies of *BRCA1* c.5339T>C (p.L1780P) mutation solely from the tumor cells. The protein level of BRCA1 in SBP77 PDXDC exhibited an approximately 50% reduction compared to the *BRCA1* wild-type cell line, MDA-MB-231, as typically expected in LOH cases (Figure S5).

BRCA1 L1780P is highly associated with HRD

Next, we investigated whether the two *BRCA1* L1780P mutant exhibit HRD. To estimate the HRD status, we utilized two widely used HRD prediction methods: HRDetect[30,31] and CHORD.[32] These methods rely on various genomic features, including HRD score, LOH status, specific single base substitution signatures, large structural variants (SVs), and deletion with microhomology to model the sequencing data with HRD. Both methods have been well established and demonstrated respectable prediction performance in assessing HRD status in various cancer samples.[31–33]

Both primary tumor samples, SBP60 Primary and SBP77 Primary, exhibited extremely high HRDetect scores (0.96 and 0.99, respectively), which remained consistent in the corresponding PDX models, despite the presence of LOH (SBP60) and reversion (SBP77) of *BRCA1* gene

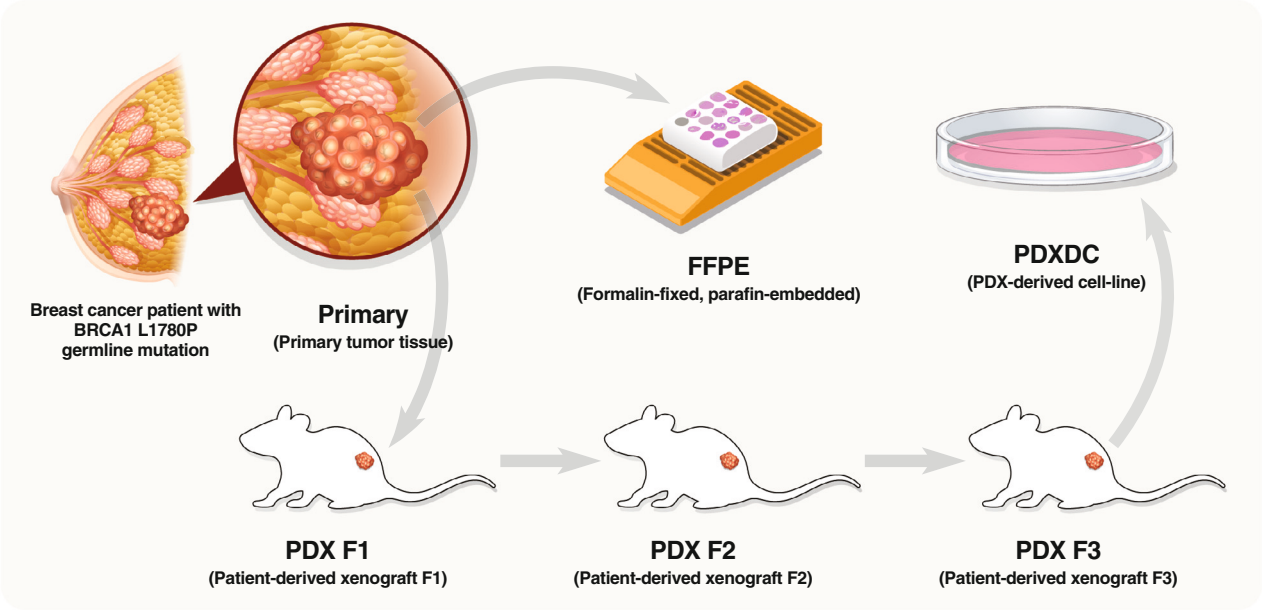

Figure 1. Sample preparation

Schematic illustration of sample preparation. The sample naming in this study follows the denotation as presented in this figure.

(Figure 3A). The HRDetect scores of these SBP samples were compared to those of other breast cancer samples (n = 566) reported by Nik-Zainal et al.[34] Among 568 breast cancer samples, 128 (22.54%) exceeded the HRD threshold (HRDectect score >0.7), including SBP60 and SBP77 (Figure S6). Notably, among the subset of 125 samples harboring any type of *BRCA1* germline mutation,[31] only 51.2% of *BRCA1* mutant samples (64/125) exceeded the HRD threshold (Figure 3B). A consistent result was observed when examining the HRD score,[35] which is previously developed HRD measuring algorithm and one of the features of HRDetect. All of the BRCA1 L1780P mutant samples exceeded the HRD threshold (HRD-sum >42, Figure S7). This finding suggests that while not all *BRCA1* mutants exhibit HRD, the L1780P mutation shows significant correlation with high HRDetect score compared to the random *BRCA1* mutation (p = 0.01326, Fisher's exact test).

The CHORD probabilities of both samples also indicate a high likelihood of HRD, with probabilities of 0.86 for SBP60 and 0.89 for SBP77 (Figure 3C). CHORD predicts HRD and classifies whether the HRD pattern is attributed to *BRCA1* or *BRCA2* deficiency. Intriguingly, both patients, having SBP77 with a damaging germline mutation in *BRCA2*, exhibited a *BRCA1*-type HRD pattern. Furthermore, we compared the CHORD probabilities of the L1780P samples with a cohort of 108 pan-cancer patients with *BRCA1* pathogenic mutations, as reported by Nguyen et al.[32] and confirmed that the L1780P samples belonged to the high CHORD probability group among 114 *BRCA1* pathogenic mutants (Figure 3D).

The combined results from HRDetect and CHORD analyses provide valuable insights into the HRD status of *BRCA1* L1780P mutants, suggesting that this particular mutation may play a significant role in driving HRD-related phenotypes in breast cancer and potentially inform treatment strategies and personalized therapeutic approaches for patients with breast cancer with this mutation.

Chemosensitivity test result unmet to the HRD prediction

HRD is often utilized as a reliable marker for predicting responses to PARPi, such as olaparib, or ATMi.[17,19,36] Based on the HRD prediction analysis, both *BRCA1* L1780P samples were expected to exhibit good sensitivity to those kinds of drugs. To validate this expectation, we conducted chemosensitivity tests using the PDX samples.

In the *in vivo* chemosensitivity test with the SBP60 PDX mouse, both olaparib and ATMi were effective in tumor regression (control vs. olaparib, p = 0.0104; control vs. AZD0156, p = 0.0106, Welch's t test, Figures 4A and 4B; Table S4). Notably, the combination treatment of olaparib and ATMi showed slightly greater tumor regression than single treatments (control vs. combination, p = 0032, Welch's t test); however, this difference was not statistically significant when directly compared to the single treatments (olaparib vs. combination, p = 0.2282; AZD0156 vs. combination, p = 0.1461, Welch's t test). To determine if the sensitivity to olaparib was specifically due to the L1780P mutation, we conducted an experiment using the *BRCA1*-null cell line HCC1937, into which we introduced either wild-type *BRCA1* or *BRCA1* L1780P via transfection. The olaparib chemosensitivity test revealed that cells transfected with *BRCA1* L1780P were more sensitive to olaparib compared to the original cell line (p = 0.0003 at 9μM treatment, Welch's t test), indicating that SBP60's sensitivity to olaparib is primarily due to presence of the L1780P mutation itself (Figure 4C; Table S5). However, the response of SBP77 PDXDC, which had a reversion mutation leaving only one copy of wild-type *BRCA1*, did not significantly differ from HCC1937$^{BRCA\ WT}$ (p = 0.0526, Welch's t test), but was significantly different from HCC1937$^{BRCA1\ L1780P}$ (p = 0.0012, Welch's t test). A similar trend was observed with ATMi treatment; the response of SBP77 PDXDC to

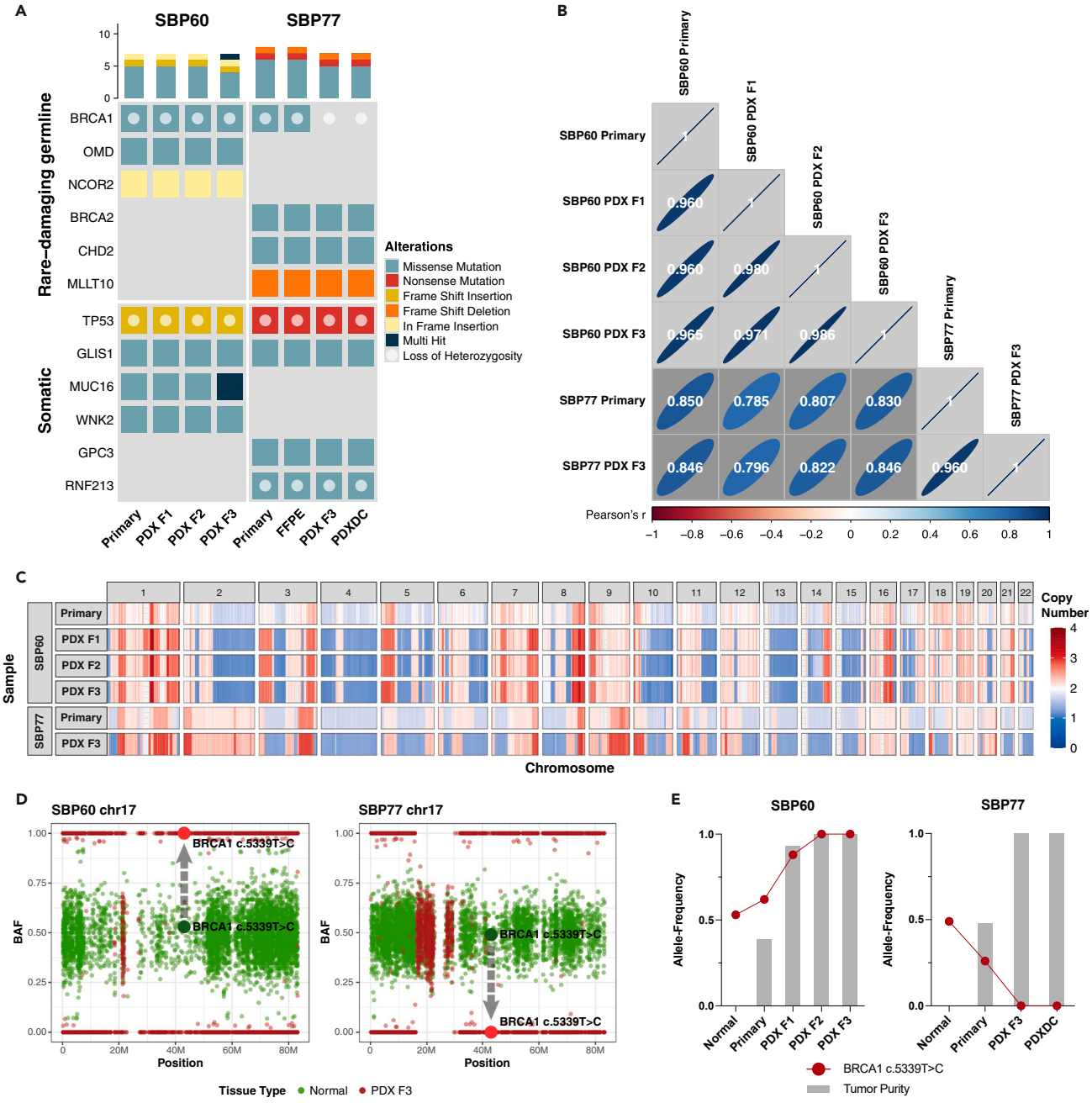

Figure 2. Genomic concordance between primary tumor tissue and PDX

(A) Rare-damaging germline mutations and somatic mutations found on primary tumor tissue and PDX samples. Only genes belonging to CGC are presented here.

(B) Gene expression concordance between the primary tumor tissue and PDX samples.

(C) Copy number status concordance between primary tumor tissue and PDX samples.

(D) The BAFs of all heterozygous SNPs on chromosome 17. Green dots represent the BAFs of heterozygous SNPs found on normal blood data, while the red dots represent BAFs of the corresponding SNPs in PDX data.

(E) Changes of *BRCA1* c.5339T>C variant allele-frequencies.

1μM ATMi was not significantly different from MDA-MB-231, a *BRCA1* proficient cell line (p = 0.1339, Welch's t test), but was significantly different from HCC1937, *BRCA1* mutant cell line (p = 0.0052, Welch's t test, Figure 4D; Table S6). Consistent results were also seen in the combination treatment (SBP77 PDXDC vs. MDA-MB-231, p = 0.0569; SBP77 PDXDC vs. HCC 1937, p = 0.0134, Welch's t test, Figure 4E;

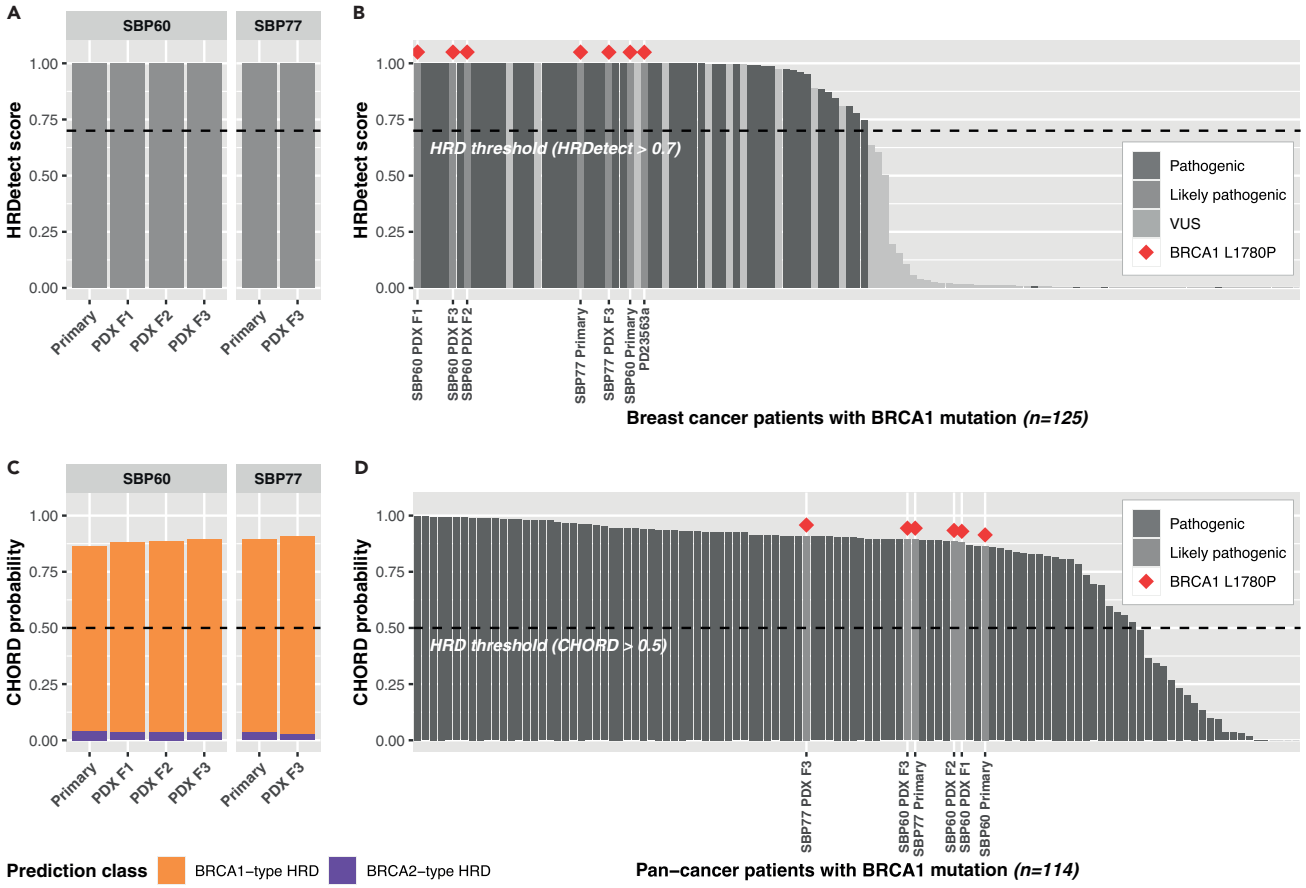

Figure 3. Prediction of homologous recombination deficiency

(A) HRDetect scores of SBP samples.

(B) HRDetect scores of SBP samples with 119 BRCA-EU samples with *BRCA1* mutations (a total of 125). One patient from BRCA-EU (PD23564a) also confirmed to harbor *BRCA1* L1780P mutation.

(C) CHORD probabilities of SBP samples (total bar height) with each bar divided into segments indicating the probability of *BRCA1*- (orange) and *BRCA2*- (purple) type HRD.

(D) CHORD probabilities of SBP samples of 108 patients with pancreatic cancer with *BRCA1* pathogenic mutations (a total of 114).

Table S7). These results suggest that the reversion mutation can lead to resistance to HR-targeting drugs, despite having a high HRD prediction score. Therefore, when utilizing HRD prediction to predict drug response, comprehensive evaluation of LOH and reversion status is crucial when using HRD prediction to anticipate drug response.

In summary, our *in vivo* and *in vitro* chemosensitivity tests using PDX samples confirmed that PARPi and ATMi are effective drugs for treating *BRCA1* L1780P mutant cancer. However, an important finding from our study is the potential impact of reversion mutations on drug response. We observed that in cases where reversion occurred, despite having a high HRD prediction score, the homologous recombination machinery appeared to be restored, leading to the acquisition of drug resistance.

DISCUSSION

To comprehensively investigate the characteristics of the *BRCA1* L1780P mutation, we utilized two PDX models and established a PDXDC. Through WGS, WES, and RNA sequencing, we conducted genomic analyses to elucidate the molecular landscape of these tumors. The genomic landscape of the primary tumors was remarkably well-preserved in their corresponding PDX models. Notably, variants that initially had a variant allele frequency (VAF) in the primary tumors exhibited a significant increase in VAF as tumor purity improved in the PDX samples. This advantage of enhanced tumor purity was also evident in the analysis of copy number alterations and LOH. The increased tumor purity played a crucial role in identifying and confirming the reversion mutation of *BRCA1* L1780P. Moreover, we explored the conservation of gene expression patterns in the PDX models. Concerns regarding potential alterations in gene expression patterns in PDX have been raised by many researchers.[37–39] However, our study demonstrates that the transcriptional characteristics are indeed extremely well conserved in PDX, providing confidence in the reliability of gene expression data obtained from PDX models. Overall, PDX models offer a controlled and enriched environment for tumor growth, resulting in higher tumor purity with conserved genetic characteristics of primary tumors. These advantages make PDX models a valuable preclinical tool for patient profiling.

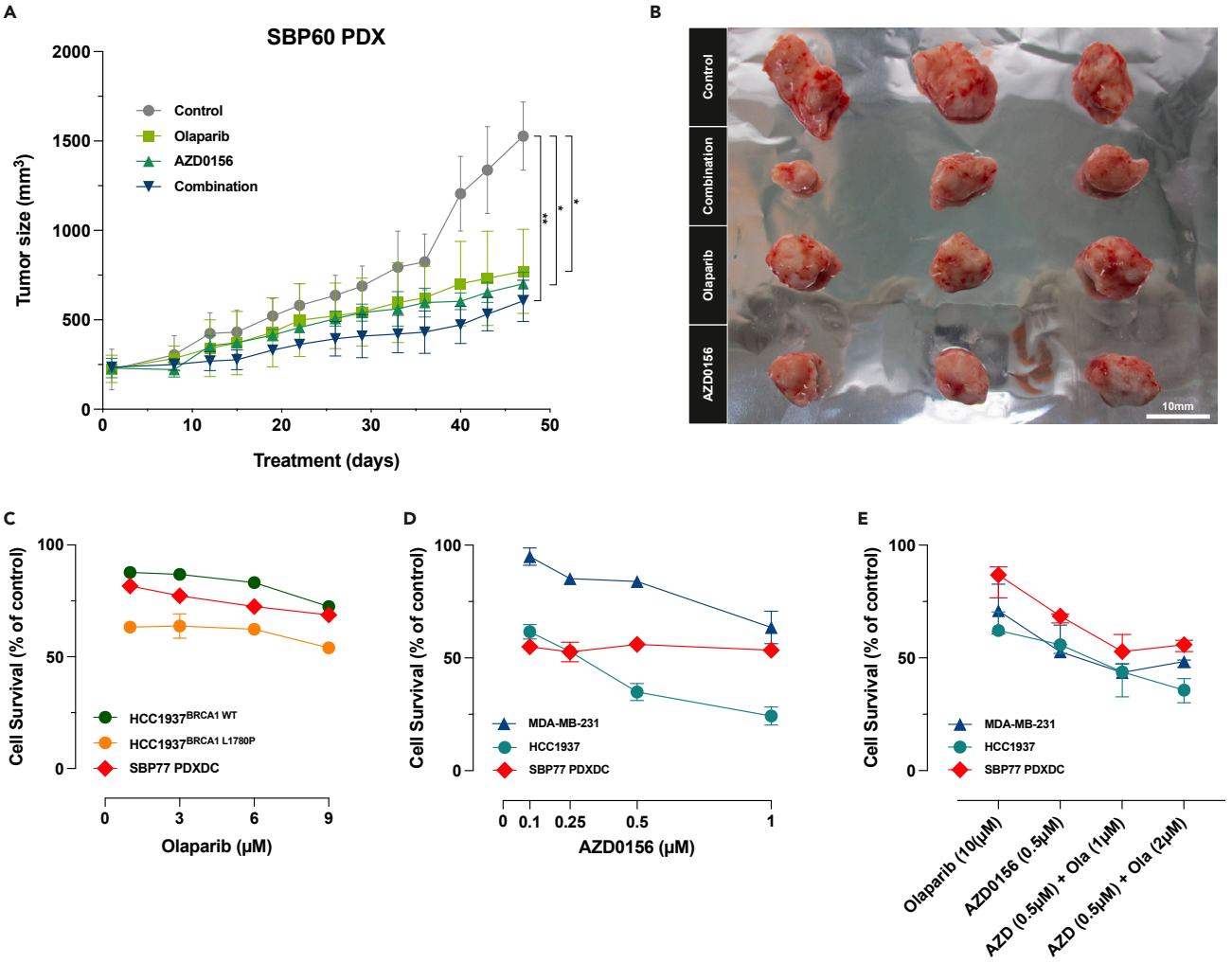

Figure 4. Chemosensitivity test of PAPRi and ATMi

(A and B) Tumor sizes observed upon olaparib (PARPi) and AZD0156 (ATMi) treatment on SBP60 PDX mouse. (Scale bar represents 10mm).

(C) Olaparib chemosensitivity test with cell lines.

(D) AZD0156 chemosensitivity test with cell lines.

(E) Chemosensitivity test for the combination treatment of olaparib and AZD0156. Data are presented as means ± SDs. Error bars are omitted when the error range is smaller than the size of the data point.

In the current study, we performed both *in vivo* and *in vitro* drug-sensitivity tests using PDX, PDXDC, and commercial TNBC cell lines. Interestingly, significant tumor regression was observed when these models were treated with a combination of PARPi and ATMi, indicating the potential effectiveness of this combination strategy for patients with the L1780P mutation. Similar to other mutations within the BRCT domain, the L1780P mutation appears to damage the BRCT domain, leading to disrupted activation of the HR signaling cascade.[40–42] This disruption may contribute to the high sensitivity of L1780P mutant tumors to PARPi and ATMi.[17–19]

We observed a unique case of LOH resulting in the reversion of the *BRCA1* L1780P mutation in SBP77. In patients with breast cancer, determining the HRD status holds immense potential for tailoring personalized treatment strategies. Methods like HRDetect[30,31] or CHORD,[32] which predict HRD status, offer significant clinical benefits. However, our findings suggest that in cases of reversion mutations, there may be a slight recovery of the homologous recombination machinery, leading to resistance against HR-targeting drugs.[43] Despite the presence of genetic damage, HRD prediction could still remain high. This highlights the importance of vigilant monitoring and thoughtful consideration of reversion mutations when designing treatment plans for patients with breast cancer with *BRCA1/2* mutations.

The resistance to PARPi and ATM indicates that the homologous recombination may be partially restored when a reversion mutation occurs. Pettitt et al. have well documented this phenomenon in their study,[43] which includes over 300 cases where reversion mutations. They report that reversions in *BRCA1* and *BRCA2* are strongly correlated with resistance to PARPi and platinum drugs, noting that reversion of missense mutations is relatively rare compared to more severe mutations like frameshift or nonsense mutations, which underscores the significance of our study.

Although fully elucidating the mechanism behind this restoration is beyond the scope of this study, existing literature provides some insights into potential mechanisms. For instance, Vaclová et al. suggested that *BRCA1* missense variants in the BRCT domain might exert a dominant-negative effect, inhibiting the function of wild-type *BRCA1*.[44] In cases where a deletion includes the mutant *BRCA1* allele (reversion mutation), the dominant mutated *BRCA1* are no longer transcribed, which could lead to the restoration of homologous recombination. This restoration may contribute to resistance to PARPi or ATMi. However, it is crucial to recognize that the specific effects of mutated *BRCA1* on wild-type *BRCA1* function can vary depending on factors such as the genomic locus of the mutation or the type of mutation. Therefore, it is challenging to conclusively determine the mechanism behind drug resistance at this stage. Further research is needed to fully elucidate these mechanisms.

Our study provides valuable insights into the genomic characteristics and therapeutic implications of the *BRCA1* L1780P mutation in breast cancer. Through the establishment of PDX models and PDXDC, we could comprehensively explore the molecular landscape of tumors harboring this specific mutation. Our genomic analyses revealed that the *BRCA1* L1780P mutation induces dysfunction of the gene, leading to impaired DNA repair mechanisms and the accumulation of genomic instability. Interestingly, we observed opposite cases of LOH, resulting in the reversion of the *BRCA1* L1780P mutation, which can impact the sensitivity of tumors to HRD-targeting drugs. Based on *in vivo* and *in vitro* drug-sensitivity tests, we demonstrated that the combination treatment of olaparib and ATMi could effectively induce tumor regression. However, caution is warranted as we observed that the occurrence of reversion mutations can lead to restored HR functions and the development of resistance to HRD-targeting drugs, despite the HRD prediction scores may be high.

Overall, our study highlights the clinical relevance of the *BRCA1* L1780P mutation and provides valuable information for guiding therapeutic approaches in patients with breast cancer with this mutation.

Limitations of the study

The findings of this study are primarily based on a limited set of PDX models and cell lines, which restricts the broader applicability of the results. The scarcity of this specific mutation poses a significant challenge in gathering enough cases for a robust analysis. Including a larger and more diverse set of tissue samples in future studies would enhance our understanding of the genomic dynamics and drug responses associated with this mutation.

STAR★METHODS

Detailed methods are provided in the online version of this paper and include the following:

- KEY RESOURCES TABLE
- RESOURCE AVAILABILITY
  - Lead contact
  - Materials availability
  - Data and code availability
- EXPERIMENTAL MODEL AND STUDY PARTICIPANT DETAILS
  - Cell culture
  - Generation of patient-derived xenograft (PDX) and PDX-derived cell line models
- METHOD DETAILS
  - Sequencing data generation
  - Gene expression concordance analysis
  - Single nucleotide variant (SNV), insertion and deletion (INDEL) calling
  - Copy number calling and tumor purity estimation
  - Prediction of homologous recombination deficiency
  - Western blot
  - Polymerase chain reaction (PCR)
  - Cell proliferation assay
  - Chemosensitivity test in PDX models
- QUANTIFICATION AND STATISTICAL ANALYSIS

SUPPLEMENTAL INFORMATION

Supplemental information can be found online at https://doi.org/10.1016/j.isci.2024.110469.

ACKNOWLEDGMENTS

This work was supported by the Basic Science Research Program through the National Research Foundation of Korea funded by the Ministry of Education (grant number 2016R1D1A1B03934564); the AZ-KHIDI Oncology Research Program (2017), the National Research Foundation of Korea funded by the Korea government (MSIT) (grant number 2022R1C1C1010441); Bio&Medical Technology Development Program, the National Research Foundation funded by the Korean government (MSIT) (grant number RS-2023-00261820); Postdoctoral Training Support

Program, the National Research Foundation funded by the Korean government (MSIT) (grant number RS-2023-00272621); and a faculty research grant of Yonsei University College of Medicine (grant number 6-2021-0239).

AUTHOR CONTRIBUTIONS

Conceptualization, H.S.P., S.K., J.D.L., and S.-Y.J.; methodology, J.D.L. and S.-Y.J.; investigation, J.D.L., S.-Y.J., J.W., and J.P.; resources, J.S. and S.-I.K.; validation, J.D.L. and T.K.; writing – original draft, S.-Y.J. and J.D.L; writing – review & editing, S.-Y.J., J.D.L., H.S.P., and S.K; visualization, S.-Y.J. and J.D.L.; supervision, H.S.P. and S.K.; funding acquisition, H.S.P., S.K., and S.-Y.J.

DECLARATION OF INTERESTS

S. Kim is cofounder of AIMA Inc., which seeks to develop techniques for early cancer diagnosis based on circulating tumor DNA.

Received: February 19, 2024
Revised: May 12, 2024
Accepted: July 3, 2024
Published: July 6, 2024

REFERENCES

1. Sung, H., Ferlay, J., Siegel, R.L., Laversanne, M., Soerjomataram, I., Jemal, A., and Bray, F. (2021). Global Cancer Statistics 2020: GLOBOCAN Estimates of Incidence and Mortality Worldwide for 36 Cancers in 185 Countries. CA. Cancer J. Clin. *71*, 209–249. https://doi.org/10.3322/caac.21660.
2. Harbeck, N., Penault-Llorca, F., Cortes, J., Gnant, M., Houssami, N., Poortmans, P., Ruddy, K., Tsang, J., and Cardoso, F. (2019). Breast cancer. Nat. Rev. Dis. Primers *5*, 66. https://doi.org/10.1038/s41572-019-0111-2.
3. Dent, R., Trudeau, M., Pritchard, K.I., Hanna, W.M., Kahn, H.K., Sawka, C.A., Lickley, L.A., Rawlinson, E., Sun, P., and Narod, S.A. (2007). Triple-negative breast cancer: clinical features and patterns of recurrence. Clin. Cancer Res. *13*, 4429–4434. https://doi.org/10.1158/1078-0432.Ccr-06-3045.
4. Cleator, S., Heller, W., and Coombes, R.C. (2007). Triple-negative breast cancer: therapeutic options. Lancet Oncol. *8*, 235–244. https://doi.org/10.1016/s1470-2045(07)70074-8.
5. Foulkes, W.D., Smith, I.E., and Reis-Filho, J.S. (2010). Triple-negative breast cancer. N. Engl. J. Med. *363*, 1938–1948. https://doi.org/10.1056/NEJMra1001389.
6. Schneider, B.P., Winer, E.P., Foulkes, W.D., Garber, J., Perou, C.M., Richardson, A., Sledge, G.W., and Carey, L.A. (2008). Triple-negative breast cancer: risk factors to potential targets. Clin. Cancer Res. *14*, 8010–8018. https://doi.org/10.1158/1078-0432.Ccr-08-1208.
7. Lehmann, B.D., Bauer, J.A., Chen, X., Sanders, M.E., Chakravarthy, A.B., Shyr, Y., and Pietenpol, J.A. (2011). Identification of human triple-negative breast cancer subtypes and preclinical models for selection of targeted therapies. J. Clin. Invest. *121*, 2750–2767. https://doi.org/10.1172/jci45014.
8. Kalimutho, M., Parsons, K., Mittal, D., López, J.A., Srihari, S., and Khanna, K.K. (2015). Targeted Therapies for Triple-Negative Breast Cancer: Combating a Stubborn Disease. Trends Pharmacol. Sci. *36*, 822–846. https://doi.org/10.1016/j.tips.2015.08.009.
9. Gonzalez-Angulo, A.M., Timms, K.M., Liu, S., Chen, H., Litton, J.K., Potter, J., Lanchbury, J.S., Stemke-Hale, K., Hennessy, B.T., Arun, B.K., et al. (2011). Incidence and outcome of BRCA mutations in unselected patients with triple receptor-negative breast cancer. Clin. Cancer Res. *17*, 1082–1089. https://doi.org/10.1158/1078-0432.Ccr-10-2560.
10. Sorlie, T., Tibshirani, R., Parker, J., Hastie, T., Marron, J.S., Nobel, A., Deng, S., Johnsen, H., Pesich, R., Geisler, S., et al. (2003). Repeated observation of breast tumor subtypes in independent gene expression data sets. Proc. Natl. Acad. Sci. USA *100*, 8418–8423. https://doi.org/10.1073/pnas.0932692100.
11. Foulkes, W.D., Brunet, J.S., Stefansson, I.M., Straume, O., Chappuis, P.O., Bégin, L.R., Hamel, N., Goffin, J.R., Wong, N., Trudel, M., et al. (2004). The prognostic implication of the basal-like (cyclin E high/p27 low/p53+/glomeruloid-microvascular-proliferation+) phenotype of BRCA1-related breast cancer. Cancer Res. *64*, 830–835. https://doi.org/10.1158/0008-5472.can-03-2970.
12. Venkitaraman, A.R. (2002). Cancer susceptibility and the functions of BRCA1 and BRCA2. Cell *108*, 171–182. https://doi.org/10.1016/s0092-8674(02)00615-3.
13. Gudmundsdottir, K., and Ashworth, A. (2006). The roles of BRCA1 and BRCA2 and associated proteins in the maintenance of genomic stability. Oncogene *25*, 5864–5874. https://doi.org/10.1038/sj.onc.1209874.
14. Lips, E.H., Mulder, L., Oonk, A., van der Kolk, L.E., Hogervorst, F.B., Imholz, A.L., Wesseling, J., Rodenhuis, S., and Nederlof, P.M. (2013). Triple-negative breast cancer: BRCAness and concordance of clinical features with BRCA1-mutation carriers. Br. J. Cancer *108*, 2172–2177. https://doi.org/10.1038/bjc.2013.144.
15. Turner, N., Tutt, A., and Ashworth, A. (2004). Hallmarks of 'BRCAness' in sporadic cancers. Nat. Rev. Cancer *4*, 814–819. https://doi.org/10.1038/nrc1457.
16. Bianchini, G., Balko, J.M., Mayer, I.A., Sanders, M.E., and Gianni, L. (2016). Triple-negative breast cancer: challenges and opportunities of a heterogeneous disease. Nat. Rev. Clin. Oncol. *13*, 674–690. https://doi.org/10.1038/nrclinonc.2016.66.
17. Zhou, J., Gelot, C., Pantelidou, C., Li, A., Yücel, H., Davis, R.E., Färkkilä, A., Kochupurakkal, B., Syed, A., Shapiro, G.I., et al. (2021). A first-in-class Polymerase Theta Inhibitor selectively targets Homologous-Recombination-Deficient Tumors. Nat. Cancer *2*, 598–610. https://doi.org/10.1038/s43018-021-00203-x.
18. Leibowitz, B.D., Dougherty, B.V., Bell, J.S.K., Kapilivsky, J., Michuda, J., Sedgewick, A.J., Munson, W.A., Chandra, T.A., Dry, J.R., Beaubier, N., et al. (2022). Validation of genomic and transcriptomic models of homologous recombination deficiency in a real-world pan-cancer cohort. BMC Cancer *22*, 587. https://doi.org/10.1186/s12885-022-09669-z.
19. Hopkins, J.L., Lan, L., and Zou, L. (2022). DNA repair defects in cancer and therapeutic opportunities. Genes Dev. *36*, 278–293. https://doi.org/10.1101/gad.349431.122.
20. Park, J.S., Nam, E.J., Park, H.S., Han, J.W., Lee, J.Y., Kim, J., Kim, T.I., and Lee, S.T. (2017). Identification of a Novel BRCA1 Pathogenic Mutation in Korean Patients Following Reclassification of BRCA1 and BRCA2 Variants According to the ACMG Standards and Guidelines Using Relevant Ethnic Controls. Cancer Res. Treat. *49*, 1012–1021. https://doi.org/10.4143/crt.2016.433.
21. Park, H.S., Lee, J.D., Kim, J.Y., Park, S., Kim, J.H., Han, H.J., Choi, Y.A., Choi, A.R., Sohn, J.H., and Kim, S.I. (2019). Establishment of chemosensitivity tests in triple-negative and BRCA-mutated breast cancer patient-derived xenograft models. PLoS One *14*, e0225082. https://doi.org/10.1371/journal.pone.0225082.
22. Lee, J.D., Ryu, W.J., Han, H.J., Kim, T.Y., Kim, M.H., and Sohn, J. (2022). Molecular Characterization of BRCA1 c.5339T>C Missense Mutation in DNA Damage Response of Triple-Negative Breast Cancer. Cancers *14*, 2405. https://doi.org/10.3390/cancers14102405.
23. Ryu, J.M., Kang, G., Nam, S.J., Kim, S.W., Yu, J., Lee, S.K., Bae, S.Y., Park, S., Paik, H.J., Kim, J.W., et al. (2017). Suggestion of BRCA1 c.5339T>C (p.L1780P) variant confer from 'unknown significance' to 'Likely pathogenic' based on clinical evidence in Korea. Breast *33*, 109–116. https://doi.org/10.1016/j.breast.2017.03.006.
24. Jung, J., Seol, H.S., and Chang, S. (2018). The Generation and Application of Patient-Derived Xenograft Model for Cancer Research. Cancer Res. Treat. *50*, 1–10. https://doi.org/10.4143/crt.2017.307.
25. Hidalgo, M., Amant, F., Biankin, A.V., Budinská, E., Byrne, A.T., Caldas, C., Clarke,

R.B., de Jong, S., Jonkers, J., Mælandsmo, G.M., et al. (2014). Patient-derived xenograft models: an emerging platform for translational cancer research. Cancer Discov. *4*, 998–1013. https://doi.org/10.1158/2159-8290.Cd-14-0001.

26. Tentler, J.J., Tan, A.C., Weekes, C.D., Jimeno, A., Leong, S., Pitts, T.M., Arcaroli, J.J., Messersmith, W.A., and Eckhardt, S.G. (2012). Patient-derived tumour xenografts as models for oncology drug development. Nat. Rev. Clin. Oncol. *9*, 338–350. https://doi.org/10.1038/nrclinonc.2012.61.
27. Siolas, D., and Hannon, G.J. (2013). Patient-derived tumor xenografts: transforming clinical samples into mouse models. Cancer Res. *73*, 5315–5319. https://doi.org/10.1158/0008-5472.Can-13-1069.
28. Jo, S.-Y., Kim, E., and Kim, S. (2019). Impact of mouse contamination in genomic profiling of patient-derived models and best practice for robust analysis. Genome Biol. *20*, 231. https://doi.org/10.1186/s13059-019-1849-2.
29. Chun, H., and Kim, S. (2019). BAMixChecker: an automated checkup tool for matched sample pairs in NGS cohort. Bioinformatics *35*, 4806–4808. https://doi.org/10.1093/bioinformatics/btz479.
30. Zhao, E.Y., Shen, Y., Pleasance, E., Kasaian, K., Leelakumari, S., Jones, M., Bose, P., Ch'ng, C., Reisle, C., Eirew, P., et al. (2017). Homologous Recombination Deficiency and Platinum-Based Therapy Outcomes in Advanced Breast Cancer. Clin. Cancer Res. *23*, 7521–7530. https://doi.org/10.1158/1078-0432.Ccr-17-1941.
31. Davies, H., Glodzik, D., Morganella, S., Yates, L.R., Staaf, J., Zou, X., Ramakrishna, M., Martin, S., Boyault, S., Sieuwerts, A.M., et al. (2017). HRDetect is a predictor of BRCA1 and BRCA2 deficiency based on mutational signatures. Nat. Med. *23*, 517–525. https://doi.org/10.1038/nm.4292.
32. Nguyen, L., Martens, J., W.M., Van Hoeck, A., and Cuppen, E. (2020). Pan-cancer landscape of homologous recombination deficiency. Nat. Commun. *11*, 5584. https://doi.org/10.1038/s41467-020-19406-4.
33. Štancl, P., Hamel, N., Sigel, K.M., Foulkes, W.D., Karlić, R., and Polak, P. (2022). The Great Majority of Homologous Recombination Repair-Deficient Tumors Are Accounted for by Established Causes. Frontiers in Genetics *13*, 852159. https://doi.org/10.3389/fgene.2022.852159.
34. Nik-Zainal, S., Davies, H., Staaf, J., Ramakrishna, M., Glodzik, D., Zou, X., Martincorena, I., Alexandrov, L.B., Martin, S., Wedge, D.C., et al. (2016). Landscape of somatic mutations in 560 breast cancer whole-genome sequences. Nature *534*, 47–54. https://doi.org/10.1038/nature17676.
35. Telli, M.L., Timms, K.M., Reid, J., Hennessy, B., Mills, G.B., Jensen, K.C., Szallasi, Z., Barry, W.T., Winer, E.P., Tung, N.M., et al. (2016). Homologous Recombination Deficiency (HRD) Score Predicts Response to Platinum-Containing Neoadjuvant Chemotherapy in Patients with Triple-Negative Breast Cancer. Clin. Cancer Res. *22*, 3764–3773. https://doi.org/10.1158/1078-0432.CCR-15-2477.
36. Wen, H., Feng, Z., Ma, Y., Liu, R., Ou, Q., Guo, Q., Shen, Y., Wu, X., Shao, Y., Bao, H., and Wu, X. (2022). Homologous recombination deficiency in diverse cancer types and its correlation with platinum chemotherapy efficiency in ovarian cancer. BMC Cancer *22*, 550. https://doi.org/10.1186/s12885-022-09602-4.
37. Liu, Y., Chanana, P., Davila, J.I., Hou, X., Zanfagnin, V., McGehee, C.D., Goode, E.L., Polley, E.C., Haluska, P., Weroha, S.J., and Wang, C. (2019). Gene expression differences between matched pairs of ovarian cancer patient tumors and patient-derived xenografts. Sci. Rep. *9*, 6314. https://doi.org/10.1038/s41598-019-42680-2.
38. Kim, Y., Kim, D., Cao, B., Carvajal, R., and Kim, M. (2020). PDXGEM: patient-derived tumor xenograft-based gene expression model for predicting clinical response to anticancer therapy in cancer patients. BMC Bioinf. *21*, 288. https://doi.org/10.1186/s12859-020-03633-z.
39. Offin, M., Sauter, J.L., Tischfield, S.E., Egger, J.V., Chavan, S., Shah, N.S., Manoj, P., Ventura, K., Allaj, V., de Stanchina, E., et al. (2022). Genomic and transcriptomic analysis of a diffuse pleural mesothelioma patient-derived xenograft library. Genome Med. *14*, 127. https://doi.org/10.1186/s13073-022-01129-4.
40. Yu, X., Chini, C.C., He, M., Mer, G., and Chen, J. (2003). The BRCT domain is a phospho-protein binding domain. Science *302*, 639–642. https://doi.org/10.1126/science.1088753.
41. Leung, C.C., and Glover, J.N. (2011). BRCT domains: easy as one, two, three. Cell Cycle *10*, 2461–2470. https://doi.org/10.4161/cc.10.15.16312.
42. Lee, M.S., Green, R., Marsillac, S.M., Coquelle, N., Williams, R.S., Yeung, T., Foo, D., Hau, D.D., Hui, B., Monteiro, A.N., and Glover, J.N. (2010). Comprehensive analysis of missense variations in the BRCT domain of BRCA1 by structural and functional assays. Cancer Res. *70*, 4880–4890. https://doi.org/10.1158/0008-5472.Can-09-4563.
43. Pettitt, S.J., Frankum, J.R., Punta, M., Lise, S., Alexander, J., Chen, Y., Yap, T.A., Haider, S., Tutt, A.N.J., and Lord, C.J. (2020). Clinical *BRCA1/2* Reversion Analysis Identifies Hotspot Mutations and Predicted Neoantigens Associated with Therapy Resistance. Cancer Discov. *10*, 1475–1488. https://doi.org/10.1158/2159-8290.Cd-19-1485.
44. Vaclová, T., Woods, N.T., Megias, D., Gomez-Lopez, S., Setien, F., Garcia Bueno, J.M., Macias, J.A., Barroso, A., Urioste, M., Esteller, M., et al. (2016). Germline missense pathogenic variants in the BRCA1 BRCT domain, p.Gly1706Glu and p.Ala1708Glu, increase cellular sensitivity to PARP inhibitor olaparib by a dominant negative effect. Hum. Mol. Genet. *25*, 5287–5299. https://doi.org/10.1093/hmg/ddw343.
45. Li, H. (2013). Aligning Sequence Rads, Clone Sequences and Assembly Contigs with BWA-MEM. Preprint at arXiv. https://doi.org/10.48550/arXiv.1303.3997.
46. Van der Auwera, G.A., and O'Connor, B.D. (2020). Genomics in the Cloud: Using Docker, GATK, and WDL in Terra (O'Reilly Media, Incorporated).
47. Dobin, A., Davis, C.A., Schlesinger, F., Drenkow, J., Zaleski, C., Jha, S., Batut, P., Chaisson, M., and Gingeras, T.R. (2013). STAR: ultrafast universal RNA-seq aligner. Bioinformatics *29*, 15–21. https://doi.org/10.1093/bioinformatics/bts635.
48. Ahdesmäki, M.J., Gray, S.R., Johnson, J.H., and Lai, Z. (2016). Disambiguate: An open-source application for disambiguating two species in next generation sequencing data from grafted samples. F1000Res. *5*, 2741. https://doi.org/10.12688/f1000research.10082.2.
49. Trapnell, C., Hendrickson, D.G., Sauvageau, M., Goff, L., Rinn, J.L., and Pachter, L. (2013). Differential analysis of gene regulation at transcript resolution with RNA-seq. Nat. Biotechnol. *31*, 46–53. https://doi.org/10.1038/nbt.2450.
50. Adam, M., Brandon, M., Jing, Z., and Qin, M. (2018). ViDGER: An R Package for Integrative Interpretation of Differential Gene Expression Results of RNA-Seq Data. Preprint at bioRxiv. https://doi.org/10.1101/268896.
51. Kim, S., Scheffler, K., Halpern, A.L., Bekritsky, M.A., Noh, E., Källberg, M., Chen, X., Kim, Y., Beyter, D., Krusche, P., and Saunders, C.T. (2018). Strelka2: fast and accurate calling of germline and somatic variants. Nat. Methods *15*, 591–594. https://doi.org/10.1038/s41592-018-0051-x.
52. Ha, G., Roth, A., Khattra, J., Ho, J., Yap, D., Prentice, L.M., Melnyk, N., McPherson, A., Bashashati, A., Laks, E., et al. (2014). TITAN: inference of copy number architectures in clonal cell populations from tumor whole-genome sequence data. Genome Res. *24*, 1881–1893. https://doi.org/10.1101/gr.180281.114.
53. Favero, F., Joshi, T., Marquard, A.M., Birkbak, N.J., Krzystanek, M., Li, Q., Szallasi, Z., and Eklund, A.C. (2015). Sequenza: allele-specific copy number and mutation profiles from tumor sequencing data. Ann. Oncol. *26*, 64–70. https://doi.org/10.1093/annonc/mdu479.
54. (2023). HMF Tools. https://github.com/hartwigmedical/hmftools.
55. Sztupinszki, Z., Diossy, M., Krzystanek, M., Reiniger, L., Csabai, I., Favero, F., Birkbak, N.J., Eklund, A.C., Syed, A., and Szallasi, Z. (2018). Migrating the SNP array-based homologous recombination deficiency measures to next generation sequencing data of breast cancer. NPJ Breast Cancer *4*, 16. https://doi.org/10.1038/s41523-018-0066-6.
56. Frankish, A., Diekhans, M., Jungreis, I., Lagarde, J., Loveland, J.E., Mudge, J.M., Sisu, C., Wright, J.C., Armstrong, J., Barnes, I., et al. (2021). GENCODE 2021. Nucleic Acids Res. *49*, D916–D923. https://doi.org/10.1093/nar/gkaa1087.
57. Priestley, P., Baber, J., Lolkema, M.P., Steeghs, N., de Bruijn, E., Shale, C., Duyvesteyn, K., Haidari, S., van Hoeck, A., Onstenk, W., et al. (2019). Pan-cancer whole-genome analyses of metastatic solid tumours. Nature *575*, 210–216. https://doi.org/10.1038/s41586-019-1689-y.
58. (2023). PURPLE. https://github.com/hartwigmedical/hmftools/blob/master/purple.
59. (2022). AMBER. https://github.com/hartwigmedical/hmftools/tree/master/amber.
60. (2023). COBALT. https://github.com/hartwigmedical/hmftools/tree/master/cobalt.

STAR★METHODS

KEY RESOURCES TABLE

REAGENT or RESOURCE	SOURCE	IDENTIFIER
Antibodies		
anti-BRCA1 (Human)	Bethyl Laboratories	Cat.# A300-000A; RRID: AB_67367
anti-Brca1 (Mouse)	LSBio	Cat.# LS-C314778; RRID: AB_3107033
anti-β-actin	Abclon	Cat.# AbC-2002; RRID: AB_3094668
HRP conjugated Goat anti-rabbit IgG	ENZO	Cat.# ADI-SAB-300-J; RRID: AB_11179983
Biological samples		
PDX tumor sample	Yonsei University College of Medicine	https://doi.org/10.1371/journal.pone.0225082
Chemicals, peptides, and recombinant proteins		
Olaparib (AZD2281)	Astrazeneca	N/A
ATM inhibitor (AZD0156)	Astrazeneca	N/A
RPMI 1640	Gibco	Cat.# 11875093
Fetal Bovine Serum (FBS)	Gibco	Cat.# 26140079
Penicillin/Streptomycin	Gibco	Cat.# 10378016
Protease inhibitor	Roche	Cat.# 11836153001
RIPA lysis and extraction buffer	Thermofisher Scientific	Cat.# 89900
Critical commercial assays		
CellTiter96® AQueous One Solution Cell Proliferation Assay (MTS)	Promega	Cat.# G3580
Trizol reagent	Thermofisher Scientific	Cat.# 15596018
DreamTaq Green PCR Master Mix (2X)	Thermofisher Scientific	Cat.# K1082
Pierce™ BCA Protein Assay Kits	Thermofisher Scientific	Cat.# 23225
PrimeScript™ RT Master Mix	TaKaRa	Cat.# RR036Q
Deposited data		
Raw sequencing data	This paper	SRA: PRJNA1045867
Human reference genome NCBI build 38, GRCh38	Genome Reference Consortium	http://www.ncbi.nlm.nih.gov/projects/genome/assembly/grc/human/
Experimental models: cell lines		
MDA-MB-231	ATCC	HTB-26
HCC1937	ATCC	CRL-2336
SBP77 PDXDC	Korean Cell Line Bank (Seoul National University)	N/A
HCC1937^{BRCA1WT}	Applied Biological Materials Inc. (abm)	https://doi.org/10.3390/cancers14102405
HCC1937^{BRCA1L1780P}	Applied Biological Materials Inc. (abm)	https://doi.org/10.3390/cancers14102405
Oligonucleotides		
Primer for PCR	Bioneer	N/A
Software and algorithms		
BWA-MEM	Li[45]	https://github.com/lh3/bwa
GATK	Broad Institute[46]	https://gatk.broadinstitute.org
STAR2	Dobin et al.[47]	https://github.com/alexdobin/STAR
gat	Ahdesmäki et al.[48]	https://github.com/AstraZeneca-NGS/disambiguate
BAMixchecker	Chun et al.[29]	https://github.com/heinc1010/BAMixChecker
Cuffdiff	Trapnell et al.[49]	https://github.com/cole-trapnell-lab/cufflinks

(*Continued on next page*)

Continued

REAGENT or RESOURCE	SOURCE	IDENTIFIER
VidGER	McDermaid et al.[50]	https://github.com/btmonier/vidger
Strelka2	Kim et al.[51]	https://github.com/Illumina/strelka
TitanCNA	Ha et al.[52]	https://github.com/gavinha/TitanCNA
Sequenza	Favero et al.[53]	https://bitbucket.org/sequenzatools/sequenza/
HMFtools	Hartwig Medical Foundation[54]	https://github.com/hartwigmedical/hmftools
HRDetect	Zhao et al.[30]	https://github.com/eyzhao/hrdetect-pipeline
CHORD	Nguyen et al.[32]	https://github.com/UMCUGenetics/CHORD
scarHRD	Sztupinszki et al.[55]	https://github.com/sztup/scarHRD

RESOURCE AVAILABILITY

Lead contact

Further information and requests for resources and reagents should be directed to and will be fulfilled by the lead contact, Hyung Seok Park (imgenius@yuhs.ac).

Materials availability

Patient-derived cell-lines generated in this study have been deposited to the Korean Cell Line Bank (Seoul National University, Seoul, Korea, SNU-5846F and SNU-5846H) and stable cell lines (HCC1937^{BRCA1WT} and HCC1937^{BRCA1L1780P}) generated in previous study have been deposited to Applied Biological Materials Inc. (abm, Richmond, Canada).

Data and code availability

- All sequencing data have been deposited at NCBI SRA and are publicly available as of the date of publication. Accession numbers are listed in the key resources table.
- This paper does not report original code.
- Any additional information required to reanalyze the data reported in this paper is available from the lead contact upon request.

EXPERIMENTAL MODEL AND STUDY PARTICIPANT DETAILS

Cell culture

MDA-MB-231 (HTB-26) and HCC1937 (CRL-2336) were purchased from the American Type Culture Collection (Rockville, MD, USA). Cell lines were grown in Roswell Park Memorial Institute (RPMI) 1640 medium (cat no. 11875093; ThermoFisher Scientific, Waltham, MA, USA) containing 10% fetal bovine serum (FBS) (cat no. 26140079; ThermoFisher Scientific) and 1% penicillin-streptomycin (cat no. 10378016; ThermoFisher Scientific).

We obtained PDXDCs (SNU-5846F and SNU-5846H) from PDX tumor. To establish the PDXDC, we harvested PDX tumor from SBP77 PDX and tumor was segmented into 5–10 mm^3 sections. These tumor sections were stored in the medium of RPMI1640 + 10% FBS + 1% penicillin-streptomycin and we sent tumor samples to the Korean Cell Line Bank (Seoul National University, Seoul, Korea), which attempted to establish PDXDC. Two PDXDCs (SNU-5846F and SNU-5846H) were successfully established.

In a previous study, we established stable cell lines (HCC1937^{BRCA1WT} and HCC1937^{BRCA1L1780P}) from HCC1937[22] and cells were transferred to Applied Biological Materials Inc. (abm, Richmond, Canada) according to the Cell Line License Agreement.

Cell lines were cultured at 37°C in a 5% CO2 incubator. Sub-culturing was performed when the cell confluence reached approximately 70–80% in a 100 mm dish (Corning, New York, USA). Cells were cryopreserved in cell freezing medium containing 90% FBS + 10% dimethyl sulfoxide (Duchefa Biochemie, Amsterdam, Netherlands).

Generation of patient-derived xenograft (PDX) and PDX-derived cell line models

In our previous study, we successfully established 19 PDX models of TNBC patients.[21] Among them, we attempted to establish primary cell lines from the samples with *BRCA1* L1780P, SBP60 and SBP77. Frozen passage 3 (F3) tumors of SBP60 and SBP77 (Severance Hospital, Yonsei University College of Medicine, Seoul, Korea, Table S1) were thawed and re-implanted into female NOG (NOD.Cg-Prkdcscid Il2rgtm1Sug) mice. When the tumor volume reached 1,500 mm^3, the implanted tumors were harvested from the mice under isoflurane anesthesia.

All tumor tissue was obtained with the patient's written consent and the informed written consent was provided by the patients. All procedures were approved by the Institutional Review Board of Yonsei University Health System (IRB No. 4-2012-0705). All experiments were approved by the Institutional Animal Care and Use Committee in Yonsei University Hospital System (YUHS-IACUC) and animals were maintained in a facility accredited by AAALAC International (#001071) in accordance with Guide for the Care and Use of Laboratory Animals 8th edition, NRC (2010).

METHOD DETAILS

Sequencing data generation

For the genomic and transcriptomic analysis, we generated whole genome sequencing (WGS), whole exome sequencing (WES), and ribonucleic acid (RNA) sequencing (RNA-seq) data on every Primary and PDX bulk tissue. The WGS libraries were prepared using the TruSeq Nano DNA Sample prep kit. For WES, the SureSelectXT Human All Exon V5 library kit was used to enrich DNA within the exon regions. RNAseq was conducted using the TruSeq Stranded mRNA Sample prep kit. The PDX-derived cell line (PDXDC) and formalin-fixed, paraffin-embedded (FFPE) samples were sequenced only with WES platform. Sequenced raw reads from WGS and WES were mapped against GRCh38 human genome reference using BWA-MEM (v.0.7.17).[45] Post-processing was done with MarkDuplicate and FixMateInformation of GATK (v.4.1.9.0).[46] Sequenced raw reads from RNA-seq were mapped against GRCh38 using STAR2 aligner (2.7.3a),[47] followed by MarkDuplicate of GATK (v.4.1.9.0).[46] All sequencing data from the PDX model were processed with disambiguate (v.1.0.0)[48] to remove all the sequenced reads from murine DNA or RNA. Lastly, we employed BAMixchecker (v.1.0.1)[29] to verify whether all sequencing data originating from a single sample exhibited consistent single nucleotide polymorphisms (SNPs).

Gene expression concordance analysis

To assess the degree of similarity between the gene expressions in the tumors collected from PDX and those from primary tissues, we conducted a gene expression concordance analysis using RNAseq data. We input RNAseq BAM files and the GENECODE V43[56] gene annotation file into Cuffdiff (v2.2.1)[49] to count and normalize the aligned reads for each gene. Subsequently, we applied *vsScatterMatrix()* function from VidGER (v.1.20.0)[50] to the gene expression value matrix generated by Cuffdiff to calculate Pearson's correlation of expression values between the primary tumor tissue and the PDX tissue.

Single nucleotide variant (SNV), insertion and deletion (INDEL) calling

SNV and INDEL calling were performed using DNA data, with germline mutation calling carried out using Strelka2 (v2.9.10),[51] and somatic mutation calling conducted using Mutect2 (v2.2). For samples sequenced using the WGS and WES platforms, we performed cross validation to further verify the called variants.

Copy number calling and tumor purity estimation

Copy number alterations were estimated using the TITAN method.[52] We ran TitanCNA (v1.17.1) R package by creating hetero SNPs profile with our own script. Determination of sample purity was performed on all WGS data using Sequenza[53] and PURPLE (PURity & PLoidy Estimator, v3.8.4),[57,58] which takes B-allele frequency (BAF) values collected with AMBER (v3.9)[59] and relative read depth values calculated with COBALT (v.1.15.2).[60] The whole pipeline is available at HMF Tools github repository.[54]

Prediction of homologous recombination deficiency

HRD detection on SBP samples was performed by HRDetect[30,31] and CHORD[32] methods. For the HRDetect analysis, signature.tools.lib (v2.4.1) R package was used. Input data encompassed SNVs and indels from Mutect2, structural variants (SVs) from Manta, and allele-specific copy-number information from TitanCNA. The tool was executed with signature-type "Breast" and genome.v "hg38" option. CHORD (v2.02) was utilized to evaluate samples exhibiting *BRCA1/2*-associated HRD. The default parameters of CHORD were applied with the output vcfs from Mutect2 and Manta. To determine HRD deficiency, HRDetect applied a threshold of 0.7 while CHORD used 0.5 following each method. Additionally, HRD score was calculated with scarHRD[55] R package.

Western blot

We confirmed the *BRCA1* expression of primary cell lines from the SBPDX77 tumor. *BRCA1* wild-type cell line (MDA-MB-231) and *BRCA1* mutant cell line (HCC1937) were used to compare the expression level of *BRCA1*. Protease inhibitor (cat.no 11836153001; Loche, Basel, Switzerland) was added to RIPA lysis and extraction buffer (cat.no 89900; ThermoFisher Scientific, Waltham, MA) and protein was extracted from these cell lines. Protein concentration of cell lysate was quantified using a BCA protein assay kit (cat.no 23225, ThermoFisher Scientific). Moreover, 8–10% Sodium dodecyl sulfate gel was used to separate protein and transfer it to the nitrocellulose membrane (cat.no 10600003 GE Healthcare; Chicago, IL). Further, 5% skim milk was used for blocking the membrane and this membrane was stored at 4°C overnight in A300-000A antibody (LS-C314778, LSBio, mouse; Bethyl Laboratories, Montgomery, TX). Additionally, β-actin (AbC-2002; Abclon, Seoul, Korea) was used as a control. A secondary antibody (ADI-SAB-300; Farmingdale, NY) was used to detect the HRP-conjugated antibody. Imaging analysis was performed using ECL+ and ImageQuant LAS 4000 (GE Healthcare).

Polymerase chain reaction (PCR)

RNA was extracted from cell lines using TRIzol (cat.no 15596018; Thermofisher Scientific) and RNA was quantified using NanoDrop 2000/2000c (Thermofisher Scientific). cDNA was synthesized by 0.5-2μg of RNA (cat.no RR036Q; TaKaRa, Kusatsu, Japan). PCR was conducted using a PCR Master Mix (cat.no K1082; Thermofisher Scientific). *BRCA1* primers (forward-GAA ACC GTG CCA AAA GAC TTC, reverse-CCA AGG

TTA GAG AGT TGG ACA C) were used for detection. *GAPDH* primers were used as control (forward -CG ACC ACT TTG TCA AGC TCA, reverse -AG GGG AGA TTC AGT GTG GTG).

Cell proliferation assay

Stable cell lines (HCC1937^{BRCA1WT} and HCC1937^{BRCA1L1780P}), PDX-derived cell lines, MDA-MB 231, and HCC1937 cells were seeded in a 96-well plate (Corning, New York, USA) at a density of 3x10^3 cells/well. The growth rate of primary cells was measured and compared during 24–72 h. The CellTiter 96 AQueous One Solution (Promega, Madison, WI) was used to evaluate cell viability treated by olaparib (AstraZeneca, Cambridge, UK) and inhibitor (AZD0156, AstraZeneca) (ATMi) treatment. Cell proliferation assay was performed according to the manufacturer's protocol.

Chemosensitivity test in PDX models

Tumor tissues from the third generation of PDX were re-implanted into the mammary fat pad of NOD. Cg-*Prkdc*^{scid} *Il2rg*^{tm1Sug}/Jic (NOG) mice. In total, 12 mice were used in chemosensitivity tests; three mice were assigned to each group. Tumor volume was calculated twice a week by caliper (Volume = 0.5×Length×Width^2). When the tumor volume reached 200–250mm^3, olaparib and ATMi were administered by oral administration. Each drug was administered five and three times/week at doses of 50 and 2.5 mg/kg, respectively. When the average tumor volume of control reached 1,500 mm^3, euthanasia was performed by CO^2 gas inhalation.

QUANTIFICATION AND STATISTICAL ANALYSIS

Pearson's correlation shown in Figure 2B was performed using R software (v.4.3.0). Fisher's exact test, described for the BRCA1 L1780P mutant and its correlation with high HRDetect scores ($p = 0.01326$), was also calculated using R software. The actual numbers for each category are as follows: HRDetect high/BRCA1 L1780P: 7, HRDetect high/other BRCA1 mutation: 57, HRDetect low/BRCA1 L1780P: 0, HRDetect low/other BRCA1 mutation: 61. All statistical tests shown in the chemosensitivity results (Figure 4) were performed using PRISM 10 software. Three replicates for each group were used for the Welch's t-tests shown in Figures 4A–4E.